

pubs.acs.org/IECR Article

Insights into the Chemistry of the Homogeneous Thermal Oligomerization of Ethylene to Liquid-Fuel-Range Hydrocarbons

Matthew A. Conrad, Alexander Shaw, Grant Marsden, Linda J. Broadbelt,* and Jeffrey T. Miller*



Cite This: Ind. Eng. Chem. Res. 2023, 62, 2202-2216



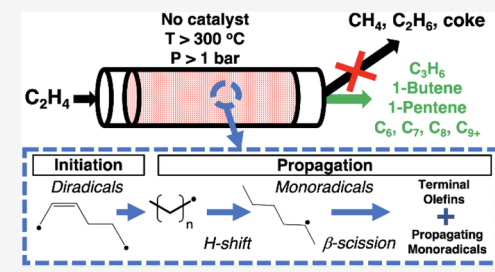
ACCESS I

Metrics & More

Article Recommendations

Supporting Information

ABSTRACT: Thermal, noncatalytic conversion of light olefins $(C_2^- - C_4^-)$ was originally utilized in the production of motor fuels at several U.S. refineries in the 1920s to 1930s. However, the resulting fuels had relatively low octane number and required harsh operating conditions (T > 450 °C, P > 50 bar), ultimately leading to its succession by solid acid catalytic processes. Despite the early utilization of the thermal reaction, relatively little is known about the reaction products, kinetics, and initiation pathway under liquid-producing conditions. In this study, thermal ethylene oligomerization was investigated near industrial operating conditions, i.e, at temperatures between 300 and 500 °C and ethylene pressures from 1.5 to 43.5 bar. Nonoligomer products such as propylene and/or higher odd carbon products



were significant at all reaction temperatures, pressures, and reaction extents. Methane and ethane were minor products (<1% each), even at ethylene conversions as high as 74%. The isomer distributions revealed a preference for linear, terminal C_4 and C_5 . The reaction order was found to be second-order with a temperature-dependent overall activation energy ranging from 39.4 to 58.3 kcal mol⁻¹. Four bimolecular initiation reaction steps for ethylene were calculated using DFT. Of these, simple H-transfer to yield vinyl and ethyl radicals was found to have a free energy activation energy barrier higher (about 10 kcal mol⁻¹) than the other three initiation steps forming either cyclobutane, 1-butene, or tetramethylene. The importance of diradical species in generating free radicals during a two-phase initiation process was proposed. The reaction chemistry for ethylene, which has only strong, vinyl C-H bonds, starkly contrasted with propylene, which possesses weaker allylic C-H bonds and showed a preference for dimeric C₆ products over C_2 – C_8 nonoligomers. The resulting C_4 and C_5 nonoligomers from propylene contained more iso-olefins compared to linear C_4 and C_5 .

1. INTRODUCTION

The U.S. shale gas boom has incentivized the on-site valorization of the residual ethane and propane that are of little value on their own. 1,2 A two-step process of alkane dehydrogenation followed by oligomerization of the resulting light olefins could be viable if the oligomerization step directly produces a fungible fuel.3 Current oligomerization processes utilize either homogeneous transition metal complexes or solid Brønsted acid catalysts.4-9 Homogeneous transition metal catalysts 10,11 can be tailored to make dimers or trimers selectively, or in the case of the Shell higher olefins process, a distribution of C₄-C₂₀ linear olefins. Y2,13 However, these processes require activators, cocatalysts, and separation units. Heterogeneous nickel ion catalysts avoid these requirements but are overall less productive, favor dimerization, and deactivate at temperatures above 250 °C.7,14 Acidic catalysts such as solid phosphoric acid (SPA)¹⁵ and zeolites, namely, H-ZSM-5, $^{16-18}$ produce liquid fuels from C_3-C_4 feedstocks; however, they tend to deactivate over time and must be regenerated.

The earliest processes for converting cracked refinery olefins were purely thermal methods dating back to the 1920s. 19-24 While the thermal reactions of olefins have been studied at atmospheric pressure since the late 1790s, 25-29 the highpressure reactions were pioneered by the work of Ipatieff in 1911.^{30,31} These high-pressure processes generally converted $C_2^{=}$ - $C_4^{=}$ feedstocks at 450-500 °C and 50-70 bar into a liquid with a research octane number (RON) of 96 and motor octane number (MON) of 78.22,23 At higher temperatures such as 650-700 °C, a highly aromatic distillate with MON of roughly 100 was demonstrated.²² In terms of productivity, Sullivan et al. achieved a liquid yield of 20.6 wt % during a contact time of 4.1 min from pure C₂H₄ at 34 bar and 453 °C in a 520 cm³ reaction bomb.²¹

The thermal route was not widely implemented due to the discovery of the CatPoly process using SPA by Ipatieff and coworkers at UOP, which produced higher-octane gasoline at lower temperatures and pressures.³² However, the thermal reaction still merits further investigation since it may confer several advantages in the modern context. For one, very little

Special Issue: In Honor of Babatunde A. Ogunnaike

June 18, 2022 Received: Revised: August 5, 2022 Accepted: August 6, 2022 Published: August 17, 2022





coking occurs, eliminating the need for frequent regenerations as in the catalytic processes. Second, the feedstock composition derived from shale gas, which is rich in ethane and subsequently ethylene, differs significantly from the typical refinery gas olefin feedstocks in the SPA process, which are composed predominantly of C_3 and C_4 . Therefore, the thermal reaction of ethylene-rich streams may capitalize on the previous observation that ethylene is the least reactive olefin with SPA, but the most reactive thermally. Studies of the thermal reactions of olefins above atmospheric pressure largely stopped after 1950. Thus, detailed product distributions and kinetics above 1 bar have not been clearly delineated, which has limited the interpretation of the reaction pathways, and thus no modeling of the reaction pathways has been reported.

The most recent adjacent studies since 1950 take place at either lower temperatures and higher pressures in the thermal polymerization to polyethylene 34-40 or at higher temperatures and lower pressures in ethylene pyrolysis from 500 to 650 °C and from 1.3 to 79 kPa in which cracking processes dominate, leading to many light gas products. 41-63 At these conditions, there is agreement across studies that propylene and ethane are major products from pure ethylene along with butenes, methane, propane, butane, butadiene, and small amounts of cyclopentene, cyclohexene, benzene, and toluene. 43-45,52, Cyclobutane has also been reported.⁶⁴ Due to the low pressures in those studies, there is very little information about the effects of temperature, pressure, and conversion on the molecular weight (MW) distribution at conditions leading to liquid fuel-range products. Furthermore, the detailed C_{4+} isomer distributions are not known. Kinetic analyses in these studies agree on a second-order ethylene pressure dependence; however, the activation energy for ethylene conversion has varied from 34.6 to 43.3 kcal mol⁻¹ across studies, with each study reporting a single value. 43-45,52,53,57,65-67 Additionally, another recurring observation among studies is an initial induction period in which the ethylene conversion rate is lower, followed by a rapid increase. This suggests the presence of a complex initiation pathway; however, no satisfactory explanation has been given, lacking any computational evidence.

The absence of rigorous quantum chemical simulations has led to differing opinions on the initiation mechanism to generate free radicals from ethylene, which unlike the higher olefins does not contain any allylic C-H bonds. Heterogeneous initiation by reactor wall effects has been ruled out by multiple studies, which found no rate enhancement by increasing the reactor surface area. 52,54,68,69 Buback suggested that the thermal polymerization of ethylene to polyethylene below 250 °C at about 2500 bar initiates via a diradical species (i.e., tetramethylene), arising from the collision of two ethylene monomers.³⁷ The diradical initiation has also been speculated in several other cases.^{39,45,70} Halstead and Quinn concluded that ethylene pyrolysis above 500 °C was controlled by the secondary decomposition of 1-butene.⁵⁴ That is, 1-butene forms initially from two ethylene via an undescribed molecular reaction and subsequently decomposes to methyl and allyl radicals that serve as the free radical chain initiators. In contrast, under similar conditions Boyd et al. asserted that the thermal reactions of ethylene initiate via a bimolecular Htransfer reaction to form vinyl and ethyl radicals, based on the claim that ethane was the only product observed initially during an induction period of several minutes.⁵²

The various initiation mechanisms proposed in literature for ethylene pyrolysis make accurate kinetic modeling challenging in the application to liquid fuel production. The goal of this study, therefore, is to better understand the reaction chemistry of the thermal reactions of ethylene at conditions conducive to producing liquid fuels: above atmospheric pressure and below pyrolytic (i.e., coking) temperatures (ca. 500 $^{\circ}\mathrm{C}$). New insights into the products and kinetics may help to advance the understanding of the key reactions and intermediates. With this aim in mind, the following four questions are posed as a broad research framework:

- (1) What are the product distributions? Notably, how does the MW distribution change as a function of temperature, pressure, and reaction conversion? What is the MW distribution at low conversion? What is the nature of the C_{4+} isomer distributions?
- (2) What are the observed kinetic parameters? That is, what are the overall activation energy and reaction order for ethylene consumption?
- (3) How do free radicals arise during the thermal initiation reactions of pure ethylene? What are the free energy barriers for possible initiation mechanisms? What are possible reactions which might lead to the propagating radical chains following initiation?
- (4) Do the thermal reactions of olefins which contain allylic C-H bonds, such as propylene and 1-hexene, behave like ethylene? Do the C_4 and C_5 product distributions share the same isomer distributions? Are the activation energy and reaction order the same? How do the overall olefin conversion rates compare?

A combination of experiments and theory was performed to explore these questions. Experimentally, the product distributions and kinetics were studied between 300 and 500 °C and from 1.5 to 43.5 bar to gain insights into the first two questions. The third question was addressed by employing density functional theory (DFT) to determine the free energy barriers for four initiation reactions previously discussed in literature but never rigorously calculated. Traditional oligomerization reactions produce even carbon chains from ethylene (i.e., butenes, hexenes, octenes, etc.). However, nonoligomer products such as propylene, pentenes, and so on were observed in significant amounts in addition to the true oligomers under all experimental conditions. Therefore, to shed light on the fourth question, the thermal reactions of propylene and 1hexene were also tested to understand their reaction chemistries under similar conditions.

2. EXPERIMENTAL METHODS

2.1. Atmospheric-Pressure Olefin Oligomerization. A quartz tube (10.5 mm ID, 1.1 mm thickness) approximately 36 cm in total length was loaded into a clamshell furnace with insulation enclosing a heated reaction zone 15 cm in length (see Figure S1). A thermal well placed down the axial length of the tube allowed the temperature profile to be measured at 2 cm intervals. A length-averaged temperature was then calculated for each temperature set point. The reactor was then heated to the desired set point and olefin flow rate. For each data point, the product gas flow rate was verified using a bubble film flow meter. Ultra-high-purity ethylene or propylene was purchased from Indiana Oxygen and used in all experiments.

Products were analyzed using a Hewlett-Packard 6890 Series Gas Chromatograph with an Agilent HP-Al/S column (25 m in length, 0.32 mm ID, and 8 μ m film thickness) and flame

Table 1. C₂H₄ Conversion in an Empty 30 cm³ Stainless-Steel Reactor at 465 °C

n (1)	15.0		25.0		21.5	
P (bar)	15.0		25.0		31.5	
flow _{feed} (sccm)	156		156		156	
$GHSV(h^{-1})$	28		17		13	
conversion (%)	21		56		74	
	Se	lectivity (Carbon %)				
methane	0.1		0.2		0.4	
ethane	0.7		0.4		0.8	
propane	0.2		0.6		1.4	
propylene	20.8		15.6		12.4	
C_4^{a}	<u>26.5</u>	(% of C ₄)	24.4	(% of C ₄)	<u>18.3</u>	(% of C ₄)
<i>n</i> -butane	0.4	(1.6%)	1.0	(4.2%)	2.2	(7.9%)
1-butene	20.0	(75.5%)	18.2	(74.4%)	12.4	(72.0%)
trans-2-butene	3.7	(14.1%)	3.2	(13.1%)	2.2	(12.2%)
cis-2-butene	2.3	(8.8%)	2.1	(8.4%)	1.4	(7.9%)
C_{5}	19.5		20.1		15.1	
C_6	13.4		15.4		13.6	
C_7	10.6		13.2		13.3	
C_8	5.3		7.9		11.4	
C_{9+}	2.9		2.2		13.3	
C_{5+}	51.7		58.7		66.7	
yield to C_{5+} (%)	11		33		49	
rate of C_2H_4 consumption (mol cm ⁻³ s ⁻¹) × 10 ⁶	1.8		4.9		6.2	
rate of C ₅₊ production (g h ⁻¹)	1.2		3.5		5.2	
^a Isobutene and isobutane were only present in tra	ace amounts (<1% each of C ₄)				

Tsobutene and isobutane were only present in trace amounts (<1% each of C_4)

ionization detector. To detect higher molecular weight products up to C_8 , the reactor discharge lines were traced with heat tape and set to 150 °C during the experiments. The conversion and product distribution were calculated on a molar basis, assuming a closed carbon balance since no significant carbon deposition was observed over the course of experiments. In experiments from 400 to 500 °C, the rates were measured at different flow rates to determine if the conversion increased proportionally with average residence time (see Figures S2a and S14), which was the case.

2.2. High-Pressure Olefin Oligomerization. To understand the product distributions and rates at higher olefin concentrations and conversions, ethylene was tested at pressures up to 43.5 bar, and propylene was tested at pressures up to 6.0 bar. A 316 stainless-steel tube (3/8 in. ID, 1/8 in. thickness) was used that was 2 feet in length, with VCR fittings at the inlet and outlet to seal the system. The reactor setup was in a ventilated fume hood as a safety precaution, and a pressure relief valve rated for 750 psi was installed at the top of the reactor. The insulation allowed a thermal reaction zone of about 42 cm which corresponded to a volume of ca. 30 cm³. A thermal well placed down the length of the tube allowed the temperature profile to be measured at 5 cm intervals (see Figure S1). A length-averaged temperature was then calculated for each temperature set point. The reactor was first pressurized to check for leaks, and then the reactor was heated to the desired set point temperature in flowing N₂ and allowed to stabilize for 4 h to purge oxygen from the system. Pure C₂H₄ or C₃H₆ was then flowed through the reactor. Ultra-high-purity ethylene or propylene, purchased from Indiana Oxygen, were used in all experiments.

Products were analyzed using a Hewlett-Packard 7890 Series Gas Chromatograph with an Agilent HP-1 column (25 m in length, 0.32 mm ID, and 8 μ m film thickness) and flame ionization detector. To detect higher molecular weight products up to C_{10} , the reactor discharge lines were traced

with heat tape and set to 175 °C during the experiment. The conversion and product distribution were calculated on a molar basis. Comparison of the product flow rate to the feed flow rate enabled an estimation of the conversion. For differential conditions (X < 10%), the product flow rate did not deviate from the expected flow rate. Additionally, very little carbon was observed over 5 days of continuous testing; thus, a 100% carbon balance was assumed in the calculations. For X >10%, the molar volumes of each carbon number group (e.g., 1hexene for C₆ products) were obtained from Yaw's Handbook,⁷¹ and the C₂H₄ conversion was estimated from the product volume flow rate. Products above C5 were assumed to be saturated in the product stream at room temperature and atmospheric pressure where the bubble flow meter was operated. In experiments above 400 °C, the rates were measured at different flow rates to determine if the conversion increased proportionally with average residence time (see Figure S2b), which was the case.

2.3. Thermal Reactions of 1-Hexene at Atmospheric Pressure. 1-Hexene (>99%) was purchased from Sigma-Aldrich, and N₂ was used as a carrier gas. Approximately 5-10 mL of 1-hexene were loaded into a roughly 100 mL stainlesssteel vessel, installed via Swagelok fittings, between the N2 mass flow controller and the reactor. The 1-hexene concentration was varied from about 1-20% in N2 at a total system pressure of about 1 bar. The reactor system was purged for 3 h with 100 sccm N₂ after sealing to purge any dissolved O2 in the 1-hexene storage vessel. The reactor effluent was fed into a gas chromatography unit equipped with a flame ionization detector. Molar selectivities of non-C6 products were reported in addition to the conversion of 1-hexene. Before the furnace was turned on, the 1-hexene was fed into the reactor at room temperature to verify no reaction due to contaminants, as well as to obtain a baseline of impurities present as received. The 1-hexene was found to be >99% pure.

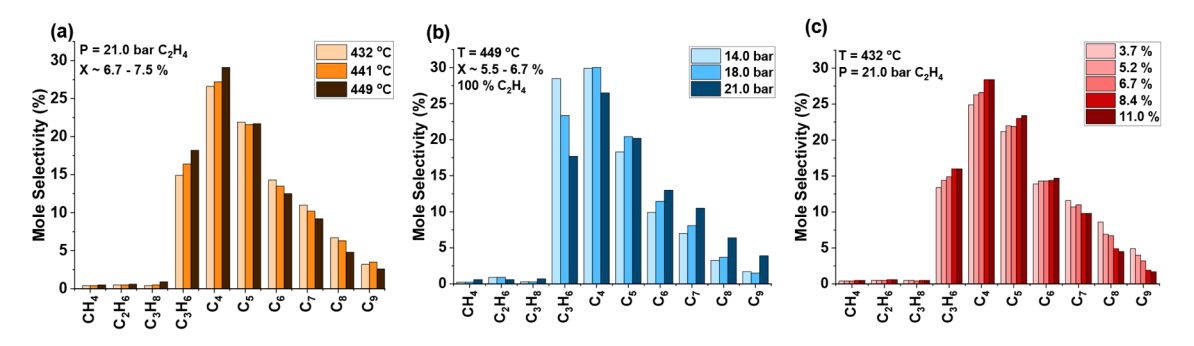


Figure 1. Product distributions of ethylene thermal reactions at high pressure: (a) 21.0 bar and ~7% conversion, temperature varied from 432 to 449 °C; (b) 449 °C and ~6% conversion, pressure varied from 14.0 to 21.0 bar; (c) 432 °C and 21.0 bar, conversion varied from 3.7 to 11.0%.

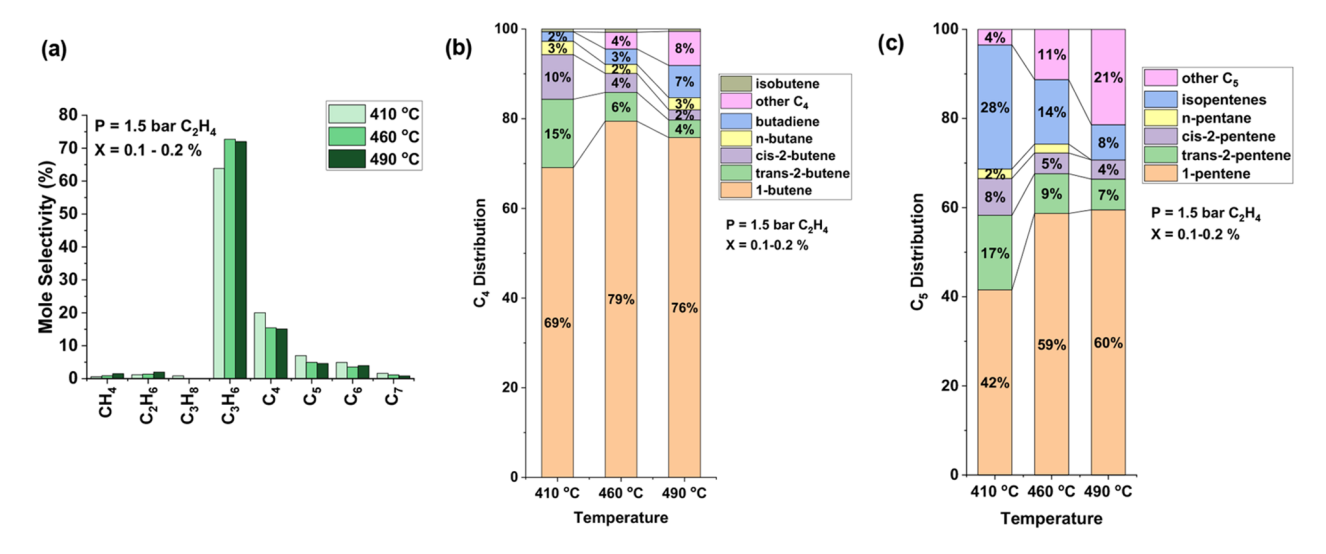


Figure 2. Product distributions at 1.5 bar C_2H_4 from 410 to 490 °C at 0.1–0.2% conversion: (a) By carbon number, (b) C_4 distribution, (c) C_5 distribution.

2.4. Computational Methods. DFT calculations were carried out using Gaussian 16⁷² to investigate ethylene oligomerization reactions. All calculations were conducted in the gas-phase using the M062X meta-hybrid functional 73,74 with the Def2-TZVP basis set of Alrichs and co-workers. The UltraFine integration grid and default optimization convergence criteria were used throughout. Dispersion was included in the form of Grimme's D3 empirical dispersion correction without any damping scheme. The correctness of each transition state was confirmed by calculation of intrinsic reaction coordinates to connect transition states to appropriate minima.

Contributions to the enthalpy of the system from frequency modes below 100 cm⁻¹ were adjusted using the quasi-harmonic (QH) correction of Head-Gordon.⁷⁷ Contributions to the entropy from the same small vibrational modes were adjusted using the QH method of Grimme.⁷⁸ Both methods were used as provided in the GoodVibes software.⁷⁹ Good-Vibes was also used to scale all vibrational frequencies by a factor of 0.971, as recommended by Truhlar et al.⁸⁰ All thermodynamic values are reported at 1 atm of pressure and at 25 °C. All minima were confirmed to have zero imaginary frequency modes, while transition states calculations showed exactly one negative frequency mode.

3. RESULTS

3.1. High Ethylene Conversion at Elevated Temperature and Pressure. As discussed in the introduction, at pressures above 1 atm, the thermal conversion of ethylene to liquid hydrocarbons occurs above about 300 °C. Given the absence of recent studies of ethylene reactions at superatmospheric conditions, high-conversion experiments were conducted in a continuous-flow stainless-steel tube reactor to determine the ethylene conversion rates and product distributions as a benchmark.

Ethylene conversions from 21 to 74% were obtained at 465 °C from 15.0 to 31.5 bar with a feed flow rate of 156 sccm in a 30 cm³ stainless-steel tube flow reactor (see Table 1). The resulting C_{5+} yield ranged from 11 to 49%. From the product analysis of ethylene reacted at 465 °C, five observations are apparent: (1) A significant yield to C_{5+} liquids (49%) was obtained at 31.5 bar. (2) Nonoligomers, such as propylene, pentenes, heptenes, and so on, comprised 50–55% of the products. (3) 1-Butene was 70–75% of the C_4 isomers, with very little isobutene or isobutane detected (<1%). (4) The gas products were highly olefinic in nature (e.g., the mole ratios of propane to propylene and butane to butenes were less than about 0.1). (5) Little methane or ethane (<1% each) was produced.

Next, the products were studied systematically over a range of temperatures, pressures, and conversions below about 10%.

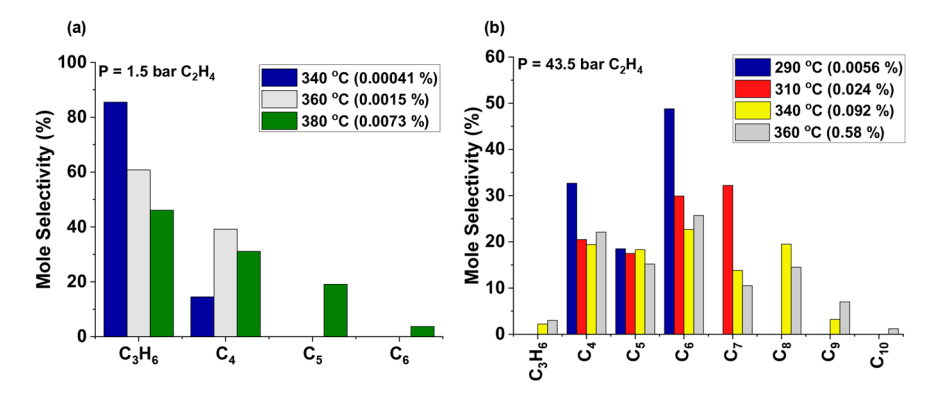


Figure 3. Product distributions for ethylene feed below 400 °C at low conversion: (a) 1.5 bar, quartz reactor with volume = 11 cm³; (b) 43.5 bar, stainless-steel reactor with volume = 30 cm³.

3.2. Effects of Temperature, Pressure, and Conversion on the MW Distribution. To understand the dependence of product distribution on changes in temperature, a series of experiments was conducted from 432 to 449 °C at 21.0 bar and ca. 7% ethylene conversion (Figure 1a). Despite being at lower pressure, temperature, and conversion than the data in Table 1, the overall product distributions shared many of the same features, with methane and ethane selectivities less than 1 mol % each, and many odd and even carbon products from C_3 to C_9 . Clearly, the selectivity to propylene and butenes increased as temperature increased, accompanied by similar decreases in C_6 to C_9 . Meanwhile, the C_5 products remained around 20 mol % at each temperature.

To probe the effect of pressure, experiments were conducted from 14.0 to 21.0 bar at 449 °C and \sim 6% ethylene conversion (Figure 1b). Changes in the reaction pressure had noticeable effects on the selectivity to propylene, C_4 , and C_6-C_9 products. As the pressure increased, selectivity to propylene and C_4 decreased commensurately with increases in C_5-C_9 . Thus, the influence of pressure appears to be opposite of the influence of increasing temperature on the C_3-C_9 distribution.

The effect of ethylene conversion up to about 10% on the product distribution was also investigated. At 21.0 bar and 432 $^{\circ}$ C, the data in Figure 1c demonstrated two key trends: (1) an increase in C₃ to C₆ fractions and (2) a corresponding relative decrease in C₇ to C₉ fractions as the conversion increased from 3.7 to 11.0%.

3.3. Isomer Distributions for C_{4+} Products. In the next series of experiments, the products were studied from 410 to 490 °C with an emphasis on understanding the C₄, C₅, and C₆ isomer distributions. Overall, in Figure 2a, at lower pressure (1.5 bar) and conversion (0.1-0.2%) than in Figure 1, propylene was the major product. However, C₄-C₇ were still produced. The C₄ distribution (Figure 2b) shows the high prevalence for linear butenes (>80%), specifically 1-butene, along with small amounts of butadiene, n-butane, and an unidentified C4. Isobutene was a very minor product, comprising less than 1% of all the C₄. The identity of the other C₄ was not confirmed, but the retention time points toward either a cyclic C₄ or isobutane. Additionally, the isomer ratios were affected by the temperature. The ratio of 1-butene to 2-butenes increased from 2.7 at 410 °C to 12.2 at 490 °C. However, the ratio of linear butenes to isobutene remained greater than 130 at all three temperatures. Furthermore, butadiene increased from 2 to 7% over the temperature range. The other C_4 similarly increased from less than 0.1% at 410 °C to 8% at 490 °C.

The C₅ distribution (Figure 2c) also shows high selectivity to linear pentenes. However, while the C₅ products were more than 65% linear, they displayed relatively more iso-olefins compared to the C₄ isomers. The branching was especially more significant at 410 °C, at which point isopentenes were 28% of C₅, but they were only 8% at 490 °C. Saturated C₅ were not major products. n-Pentane was the least abundant C5 detected (2 mol %), while isopentane was not detected. The C₅ isomers showed a temperature dependence for both the ratio of linear to branched C5 as well as the ratio of 1-pentene to 2-pentenes. The ratio of linear to branched C5 olefins increased from 2.4 at 410 °C to 8.9 at 490 °C. Likewise, the ratio of 1-pentene to 2-pentenes increased from 1.7 at 410 °C to 5.3 at 490 °C. The other C₅ isomer was observed to increase from 4 to 21% of C_5 from 410 to 490 °C. This other C_5 isomer was not determined, but each of the *n*-pentenes, isopentenes, and saturated C₅ were identified, implying that it must be either a multiply unsaturated open chain C₅ or a cyclic C₅

From the C_6 distribution, the presence of at least 10 isomers was apparent at each temperature. While most C_6 isomer identities were not assigned, the 1-hexene retention time was known from 1-hexene feed experiments. The GC data showed that 1-hexene comprised less than 5% of C_6 at each of the temperatures. Thus, the trend of high selectivity to the terminal olefin product was limited to C_4 and C_5 products.

3.4. MW Distributions at Very Low Ethylene Conversions. Pure ethylene was also reacted to determine the initial product distributions (See Figure 3a) at very low conversion. The lowest measurable conversion was 0.00041% at 340 °C and 1.5 bar. Propylene and 1-butene were the only products detected. At 380 °C and 0.0073% conversion, C_5 and C_6 products were also detected; however, propylene was the most selective product in each case. These results are somewhat surprising considering that propylene is a non-oligomer product. That is, it requires both C–C formation and C–C scission for each propylene molecule formed starting from ethylene.

Ethylene was also reacted at 43.5 bar (Figure 3b). At as low as 290 °C at the lowest measurable conversion, the only product groups detected were 1-butene, C_5 , and C_6 products. Propylene and C_{8+} products became detectable at 340 °C. At 360 °C and 0.58% conversion, there were products of each carbon number from C_3 to C_{10} , with the selectivity of each

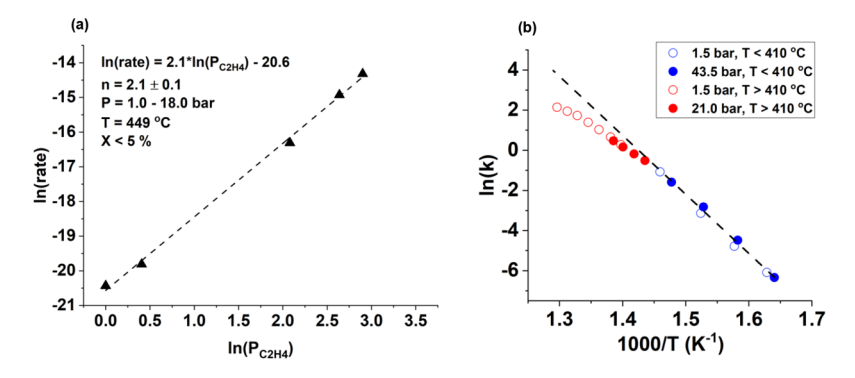


Figure 4. Kinetics of ethylene thermal reactions. Rates were measured with X < 5.0% with units of moles C_2H_4 converted cm⁻³ s⁻¹. (a) Reaction order at 449 °C from 1.0 to 18.0 bar. (b) Arrhenius plot at 1.5, 21.0, and 43.5 bar from about 340–500 °C. Rate constants are the rate normalized by the concentration using the observed 2.1 reaction order.

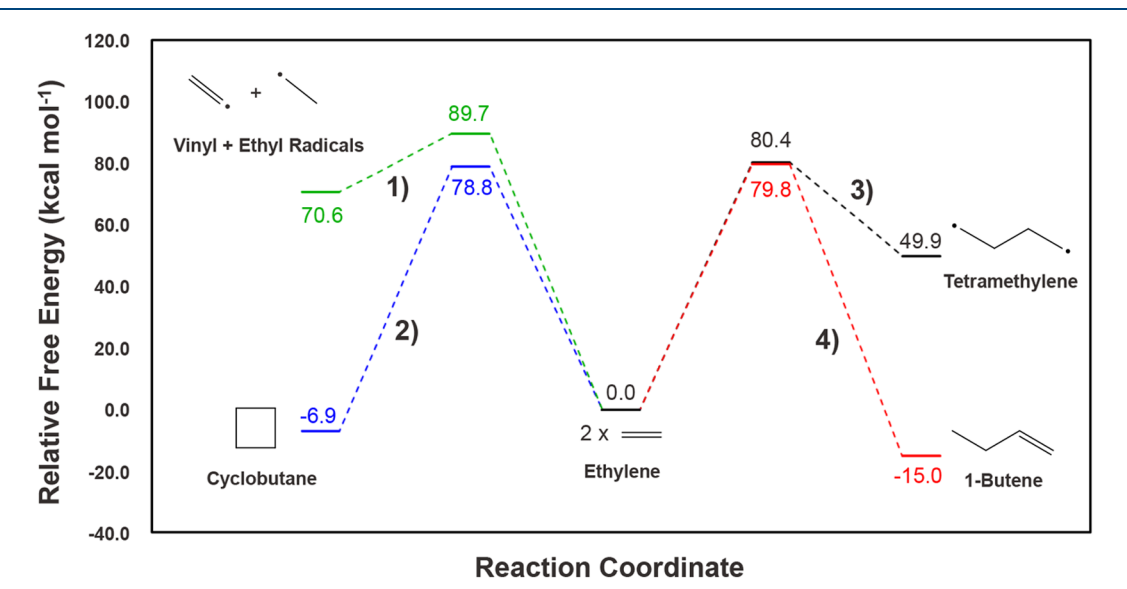


Figure 5. Free energy profiles for four bimolecular initiation reactions involving two ethylene molecules.

group decreasing from $C_6 > C_4 \sim C_8 \sim C_5 > C_7 > C_9 > C_3$. The GC chromatogram shows the quantity of distinct isomers in each carbon number group (see Figure S3). C4 consisted of about 80% 1-butene and 20% 2-butenes, in agreement with the data in Figure 2b and at high conversion in Table 1. There was an unassigned product between the C₄ and C₅ fractions. The last butene isomer, cis-2-butene, has a boiling point of 4 °C, whereas 3-methyl-1-butene and 1-pentene boil at 20 and 30 °C, respectively. However, cyclobutane boils at 12.5 °C. This product assignment, however, cannot be confirmed without a cyclobutane reference, but it would be consistent with Quick et al.'s observation that cyclobutane is formed in ethylene thermal reactions.⁶⁴ The C₅ fraction contained at least 4 isomers, about 60% of which was 1-pentene. Since there are only three possible linear pentene isomers, the data suggest that some cyclic and/or branched C₅ isomers were produced. The presence of some branched C5 was observed in Figure 2c at similar conversion, in line with this observation. C₆ appeared to have seven or more isomers. There are five possible linear C₆ isomers, so the occurrence of seven or more isomers implies the presence of cyclic and/or branched C₆ isomers. The C₇ product group increased to at least 11 isomers (with 5 possible linear C₇ isomers), which appeared highly distributed. Both C₈ and C₉ appeared to each have even more distinct isomers.

Furthermore, there was no evidence for significant amounts of saturated or doubly unsaturated products at 360 $^{\circ}$ C. Thus, even at conversions well below 0.1%, many of the product features seen at high conversion (i.e., odd carbon products, preference for 1-butene among C_4 , etc.) have already developed early in the reaction.

3.5. Measured Kinetics of the Thermal Reactions of **Ethylene.** To further understand the behavior of the thermal oligomerization of ethylene, the reaction order and activation energies were measured across a range of temperatures and pressures. Ethylene was studied from 336 to 500 °C and from 1.0 to 43.5 bar. The reaction order for ethylene was determined to be 2.1 with pressure varied from 1.0 to 18.0 bar (see Figure 4a). The Arrhenius analysis reveals a functional relationship between the activation energy and temperature. The result is the appearance of two distinct regions: a linear region below about 410 °C and a quasi-linear region above 410 °C that decreases slightly in slope with increasing temperature up to about 500 °C. The values for the low and high temperature regions are 58.3 and 39.4 kcal mol⁻¹, respectively (Figure S4). In either case, the activation energy is quite large, which is consistent with a noncatalytic gas phase reaction.

In radical chain reactions, the overall activation energy is a function of the initiation, termination, and propagation

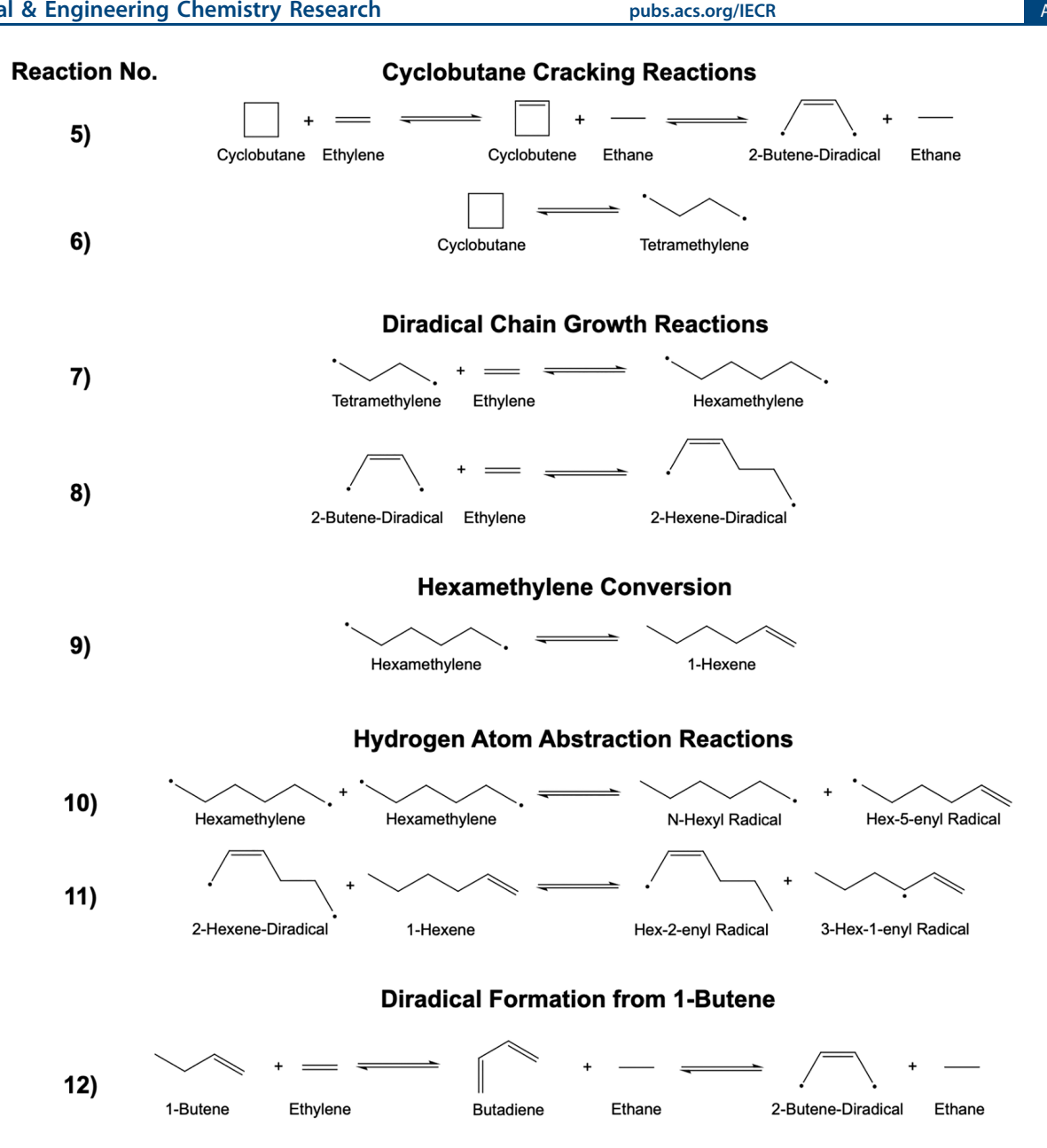


Figure 6. Secondary reactions studied following the bimolecular initiation steps (reactions 1-4 in Figure 5).

reactions. Propagation reactions in oligomerization (e.g. olefin addition or β -scission) are relatively well-known; however, the initiation steps for this reaction are not clear. In the next section, four initiation reactions were modeled to propose a reaction pathway leading to free radicals which may be used to rationalize the observed kinetics.

3.6. DFT of Proposed Initiation Reactions. To ascertain the mechanism of initiation for ethylene oligomerization, four bimolecular ethylene reactions were modeled for comparison. The relative free energies for each pathway are shown in Figure 5, alongside the products of each reaction, whereas transition states for each reaction can be seen in Figure S5. The first initiation reaction (Reaction 1, in green) is a simple hydrogen atom transfer from one ethylene molecule to another. This reaction, with a significant activation free energy of 89.7 kcal mol⁻¹, yields a vinyl and an ethyl radical. This reaction is highly endergonic, exhibiting a free energy of formation of 70.6 kcal mol⁻¹. The second pathway (Reaction 2, in blue)

concerns the formation of cyclobutane through a 2 + 2 cycloaddition reaction. This single-step reaction occurs through a highly distorted, asymmetric transition state with a large 78.8 kcal mol⁻¹ free energy barrier (see Figure S5).

Tetramethylene, as shown in black in Reaction 3, forms somewhat analogously to a standard ethylene polymerization reaction, differing in that one ethylene molecule must undergo cleavage of one C-C bond to yield a reactive dimethylene intermediate, which then attacks the other ethylene molecule. The activation barrier of 80.4 kcal mol⁻¹ for this reaction is almost identical to the cyclobutane formation; however, tetramethylene formation is considerably more endergonic due to the diradical nature of the product formed. 1-Butene formation (Reaction 4, in red) occurs through a four-centered transition state wherein a hydrogen atom from one ethylene molecule is donated to the other and the remaining vinyl moiety of the first ethylene attacks the unsaturated carbon of the second molecule. Once again, this reaction proceeds

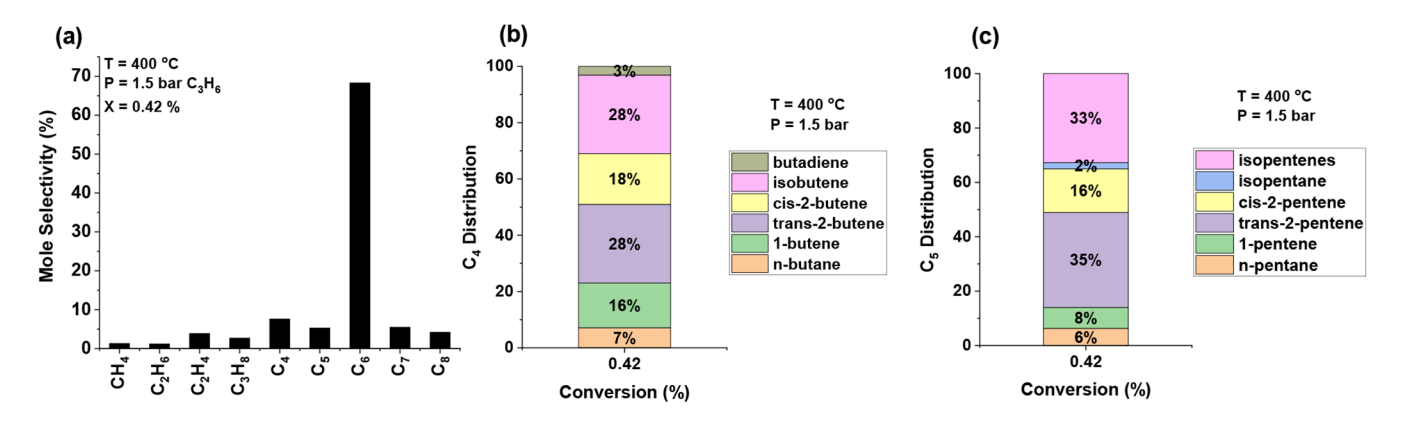


Figure 7. Product distribution at 0.42% conversion of pure propylene reacted at 1.5 bar and 400 °C by: (a) carbon number, (b) C_4 distribution, (c) C_5 distribution.

through a barrier height that is almost identical to the previous two at 79.8 kcal mol⁻¹. Unsurprisingly, the formation of 1-butene is more exergonic than cyclobutane owing to the increased degrees of freedom in the former and the ring-strain in the latter.

Next, we investigated the most feasible secondary reactions, both unimolecular and bimolecular, of the reaction products from Reactions 2–4. These three reactions had comparably lower free energy activation barriers than Reaction 1, which was the one yielding ethyl and vinyl radicals. These reactions are summarized in Figure 6 and are categorized into cyclobutane cracking, diradical chain growth, hexamethylene conversion, hydrogen atom abstraction, and 1-butene reactions

3.6.1. Cyclobutane Cracking Reactions. We identified two routes for the decomposition of cyclobutane, the first of which is shown as reaction 5 in Figure 6. Reaction 5 begins with the hydrogenation of ethylene by cyclobutane to yield cyclobutene and ethane. This cis-hydrogenation proceeds via a single symmetric transition state in which both hydrogen atoms transfer simultaneously from cyclobutane to ethylene. This reaction has a barrier height of 56.4 kcal mol⁻¹ and exhibits a minimal change in the overall free energy (Figure S6). Cleavage of the bond between the two saturated carbons of cyclobutene yields a 2-butene 1,4-diradical, and subsequent rotation of the terminal CH2 groups yields a more stable planar structure. The free energy barrier for the homolytic ringopening of cyclobutene is 56.3 kcal mol⁻¹, while rotation to the planar structure leads to a reduction in free energy of 12.6 kcal mol⁻¹. In the second mechanism, Reaction 6, formation of tetramethylene involves homolytic dissociation of a C-C bond in cyclobutane to yield a planar tetramethylene diradical. The barrier for this homolytic dissociation was calculated to be 57.1 kcal mol⁻¹ (Figure S7). Following dissociation, the tetramethylene intermediate converts to an open-book-like geometry with a C₁-C₄ dihedral angle of 60°. Rotation about the central C-C bond yields a slightly lower energy, more linear structure with a C_1 – C_4 dihedral of 175°.

3.6.2. Diradical Chain Growth Reactions. Both diradical species produced from the decomposition of cyclobutane can engage in free radical polymerization reactions with ethylene. Tetramethylene can react with ethylene to yield hexamethylene, as shown in Reaction 7, while the 2-butene 1,4-diradical species can react with ethylene to give a 2-hexene 1,6-diradical, which is Reaction 8. Addition of ethylene to either diradical occurs through a sub 20 kcal mol⁻¹ barrier. Both

pathways are also endergonic, with 2-hexene 1,4-diradical formation being slighter more free energy releasing than that of hexamethylene (see Figures S8 and S9).

3.6.3. Hexamethylene Conversion. One potential fate for the hexamethylene that is produced from the reaction of tetramethylene and ethylene is conversion to 1-hexene, as shown in Reaction 9. This reaction proceeds via an intramolecular hydrogen atom transfer, similar in nature to a retro-ene reaction. This single step pathway has a small activation free energy of 18.1 kcal mol⁻¹ and is considerably exergonic (see Figure S10), owing to the satiation of the two radical centers.

3.6.4. Hydrogen Atom Abstraction Reactions. While numerous hydrogen abstraction reactions can occur between the diradical species generated in the earlier pathways, we have chosen two possible mechanisms to focus on here. These two pathways are shown in Reactions 10 and 11. The first pathway, Reaction 10, is the transfer of a hydrogen atom from one 1hexamethylene molecule to another, yielding an *n*-hexyl radical and a hex-5-enyl radical. Formation of the two monoradical species is highly exergonic, releasing 65.6 kcal mol⁻¹ in free energy and requires a modest activation free energy of 22.7 kcal mol⁻¹ (Figure S11). The second pathway, Reaction 11, involves abstraction of an allylic hydrogen of 1-hexene to an end-chain carbon of a 2-hexene diradical. This reaction has a relatively small barrier height of 19.0 kcal mol⁻¹, as seen in Figure S12, but it is significantly less exergonic than the hydrogen atom transfer reaction between two hexamethylene molecules shown previously.

3.6.5. Diradical Formation from 1-Butene. The final pathway modeled in this work is shown in Reaction 12. It is a two-step reaction, the first step of which is the formation of butadiene and ethane from 1-butene and ethylene. This cishydrogenation is analogous to the one presented earlier in this work for cyclobutane and, unsurprisingly, has a similar free energy barrier of 54.6 kcal mol⁻¹ and reaction energy of -2.9 kcal mol⁻¹ (see Figure S13). The newly formed butadiene can then convert to a resonance stabilized diradical form, wherein the C2-C3 carbon bond has the most double bond character, and the terminal carbons are the radical centers. The free energy required for this process is 53.0 kcal mol⁻¹, lower than any other radical generating reaction step reported in this work.

3.7. Comparison to the Thermal Reactions of Other Olefins. 3.7.1. Propylene. The MW distribution of the products of the propylene reaction at 400 °C, Figure 7a,

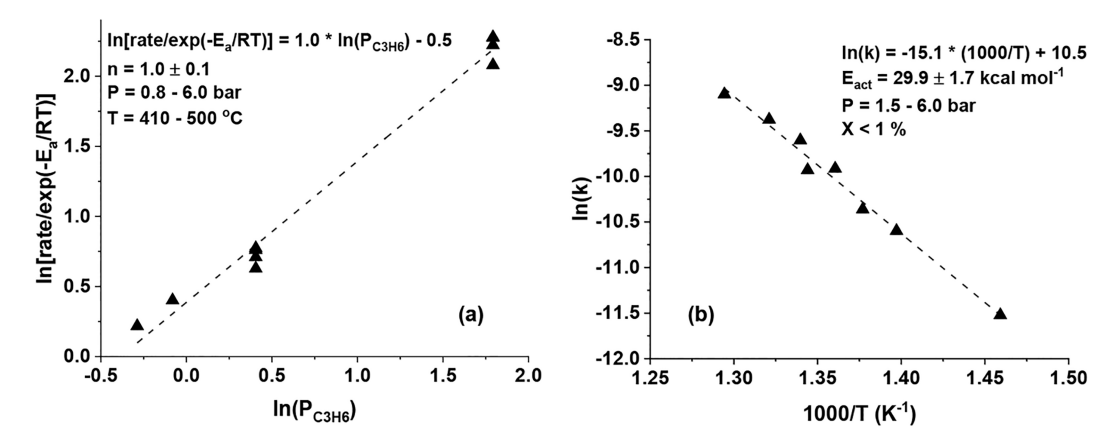


Figure 8. Kinetics of propylene thermal reactions. Rates were measured X < 1.0% with units of moles C_3H_6 converted/cm³/s. (a) Reaction order from 0.8 to 6.0 bar. Rates were normalized by the Arrhenius term $\exp(-E_a/RT)$ using the observed E_a of 29.9 kc_al mol⁻¹. (b) Arrhenius plot measured from 400 to 500 °C. Rate constants are the rate normalized by the concentration using the observed 1.0 reaction order.

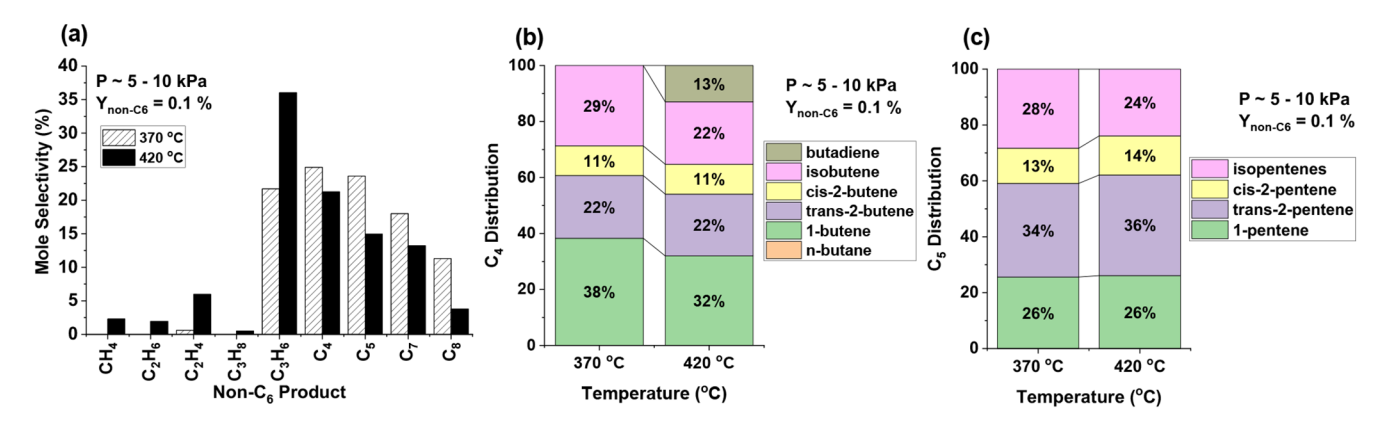


Figure 9. Product distribution of non- C_6 products at 0.1% yield to non- C_6 of 1-hexene reacted at 370 and 420 °C by (a) carbon number, (b) C_4 distribution, and (c) C_5 distribution.

shows a marked difference between the products of propylene compared with ethylene. By carbon number, the C₆ dimer is the major product (ca. 70%). Nonoligomer products were observed also (<30%), but in much smaller amounts compared to ethylene. C2, C4, C5, C7, and C8 products were detected in similar amounts (about 3-8 mol % each). Methane and ethane were present in minor amounts (less than 2 mol % each). Isobutene was 28%, and 1-butene was only 16% of the C₄. The C₅ products contained small amounts of 1-pentene (8%). There were at least 15 distinct C₆ species present at 400 °C. 1-Hexene is about 10% of the C₆, whereas several other isomers were present in larger amounts. There are 7 possible branched C₆H₁₂ isomers; therefore, a maximum of 12 open-chain olefin isomers expected. The presence of 15 isomers implies the presence of dienes, saturated C₆, and/or cyclic isomers in addition to isohexenes and *n*-hexenes.

Despite the differences in product behavior between ethylene and propylene, the effects of temperature and pressure on the products of propylene conversion, shown in Figures S15 and S16, respectively, mostly mirrored the trends seen for ethylene. Reaction at 500 °C resulted in more nonoligomers and C_1 – C_5 than at 400 °C. Meanwhile, the reaction at 6.0 bar yielded more C_{6+} products. One distinction with propylene at 500 °C was the production of more saturated products, such as methane, ethane, and propane (~20% total). Under the same conditions and reaction extent,

ethylene still produced very little amounts of saturated C_1 to C_3 (less than 4%).

The reaction order for propylene was found to be first-order from 0.8 to 6.0 bar, with an activation energy of roughly 29.9 kcal mol⁻¹ from 400 to 500 °C (see Figure 8). Thus, the kinetics of propylene compared to ethylene thermal reactions are quite distinguished, like their different product behaviors, suggesting different contributions of the possible reaction pathways.

3.7.2. 1-Hexene. The experimental results for 1-hexene are shown in Table S1. At 260 °C, no detectable conversion of 1hexene occurred. At 370 °C, 22.0% of the 1-hexene was converted. Of the products, 99.5% were seven or more C₆ isomers, and the other 0.5% were C_2 – C_8 olefins (Figure 9a). No methane, ethane, or higher paraffins were detected. Thus, thermal isomerization of 1-hexene was significant. At 400 °C and 86.0% 1-hexene conversion, 99.0% of the products were 12 or more distinct C₆ isomers (Figure S17). The remaining 1.0% of products were C2-C8 olefins, with a very small amount of methane and ethane (<1 mol % each). At 420 °C and 38.9% conversion, there was some methane and ethane (about 2.5 mol % each) in addition to the other non-C₆ olefin products (see Figure 9a). The C₄ and C₅ products from 1-hexene cracking consist of both linear and branched isomers. At 370 °C, 29% of the C₄ was isobutene, and 38% was 1-butene (Figure 9b). 1-Pentene was only 26% of C₅, and about 28% were isopentenes (Figure 9c). The appearance of about 5%

total methane and ethane at 420 °C is accompanied by butadiene, 13% of the C₄, which was not detected at 370 °C.

4. DISCUSSION

Detailed MW distributions for the thermal oligomerization of ethylene have not been reported previously above atmospheric pressure. Here, the effects of temperature, pressure, and conversion were evaluated from 14.0 to 21.0 bar and 432 to 449 °C with conversions between 3.7 and 11.0%. The temperature and pressure affect the product distribution in an opposing manner. Lower temperature and higher pressure promote the formation of longer chain products (C_{6+}) , whereas higher temperature and lower pressure result in more short-chain olefins such as propylene and 1-butene. As the reaction progresses from 3.7 to 11.0% conversion, more C_3-C_6 are produced compared to C_{7+} . It is important to note that even though the relative molar selectivity to C7-C9 decreases, the overall molar production rates of C7-C9 do not appear to decrease. These molecular weight distribution trends are thus a reflection of the propagation steps, in which C-C bond formation, leading to higher olefins such as C_{6+} , competes with C-C scission, leading to lighter olefins such as C_3H_6 and C_4 .

The occurrence of nonoligomer products such as propylene has been reported in previous studies above 500 °C at low pressure, at temperatures at which pyrolytic cracking reactions of stable olefins occur. ^{52–54,57} However, product distributions at high pressures below pyrolysis temperatures (ca. 500 °C) were all previously conducted at significant conversions above 10% but with minimal product identification. ^{19,21,22,31} This study has provided evidence that nonoligomers are present even at very low conversions below 400 °C (see Figure 2). Under these conditions at 43.5 bar and low conversion, the growth pattern does not resemble 1-carbon chain growth, despite the appearance of species with a continuous set of carbon numbers, which distinguishes it from the Fischer—Tropsch reaction. ⁸¹ Here, the competing C–C bond forming and breaking propagation reactions lead to scrambling of the MW distribution at low conversion.

This study also brings to light new information about the C₄-C₆ products. The high preference for terminal C₄ and C₅ compared to internal double bonds and branched olefins is evident. This outcome is distinct from Brønsted acid-catalyzed oligomerization, which preferentially produces internal and branched olefins, due to the higher stability of tertiary and secondary carbenium ions compared to primary carbenium ions. The stability of radicals follows the same trend (i.e., tertiary are the most stable, and primary are the least stable).⁸² Therefore, the fact that branched C₄ and C₅ olefins are minor products is evidence of a reaction pathway in which there is low preference to forming tertiary radicals. The ratios of 1butene to 2-butenes, 1-pentene to 2-pentenes, and n-pentenes to isopentenes all increased from 410 to 490 °C. Thus, temperature influences the propagation reactions in a way that leads to a stronger preference for linear, terminal C₄ and C₅ olefins at 490 °C compared to 410 °C.

The C_6 isomers deviate substantially from the C_4 and C_5 isomer distributions, which showed a strong preference to 1-butene and 1-pentene, respectively. In contrast, no individual C_6 isomer accounted for more than half of the total C_6 . In fact, at 490 °C, 1-hexene appears to be less than 5% of all C_6 , a marked difference compared to C_4 and C_5 . The same observation can be made for the C_7 – C_9 isomers at 43.5 bar

and 360 °C. More isomers are present for C_{6+} than are accounted for by the theoretical number of linear olefins, indicating that at least some skeletal isomerization and/or cyclization occurs. The ability of n-alkyl radicals to undergo 1,4- and 1,5-hydrogen-transfer reactions resulting in more stable secondary radicals is also well-known, $^{83-87}$ and it gives rise to highly branched polyethylene in the radical polymerization of ethylene. 88,89 Thus, in conjunction with the thermal isomerization of 1-hexene demonstrated in this study, the results obtained here indicate that at least two pathways exist that can lead to the diversification of isomers for C_{6+} products.

In addition to the products, the kinetics of ethylene reactions were also investigated. The previous kinetic measurements above atmospheric pressure estimated the rates from reactor pressure changes at conversions greater than 10%. 65 In the present study, the kinetic measurements were determined from conversions below 5.0% in a continuous flow reactor over a wide range of temperature and pressures. The reaction order of 2.1 obtained here agrees well with those previous studies, and DFT calculations for several proposed bimolecular initiation reactions (Figure 5) created the foundation for understanding the interplay of competing reaction pathways comprised of elementary steps on the overall observed order. 43,44,52,65,66 However, the activation energy was observed to be a function of temperature, a feature not previously reported in ethylene pyrolysis literature. Above 410 °C, the measured value, 39.4 kcal mol⁻¹, agrees with most of the values reported previously, but it increased to 58.3 kcal mol⁻¹ below 410 °C, consistent at both 1.5 and 43.5 bar. The change in activation energy with temperature is an important finding, which highlights the fact that different reaction steps can become rate controlling as the reaction conditions change. Such a feature could be captured by the application of microkinetic modeling based on a reaction mechanism comprised of the reaction families outlined here.

Free radical chain reaction pathways are well-known to be characterized by initiation, propagation, and termination reactions. Propagation and termination steps for radical chemistry are well-studied, 90,91 but the initiation step for this reaction has been under debate, lacking a rigorous energetics study.

There is strong evidence suggesting that the thermal oligomerization of ethylene proceeds first through a slow initiation stage, followed by a secondary faster period of oligomerization. ^{52,54,65} Our computational results propose several possible mechanisms that can account for a slow initiation phase, as well as more facile oligomerization reactions that are accessible through the products formed during the initiation period.

While all four of the bimolecular reactions provided in Figure 5 require significant energy input to overcome their free energy barriers, it is clear that Reaction 1, the hydrogen atom transfer reaction pathway, is considerably less favorable than the other possible routes. While the remaining three bimolecular reaction pathways exhibit similar energy requirements (Reactions 2–4), the formation of cyclobutane and of 1-butene are notably more thermodynamically favorable than tetramethylene formation. Both pathways are also reasonably exergonic, thus promoting accumulation of cyclobutane and 1-butene in the early stages of the ethylene thermal oligomerization process. For these reasons, cyclobutane and 1-butene were further explored as potential intermediates in ethylene oligomerization reactions.

Both cyclobutane decomposition pathways, Reactions 5 and 6, have comparable free energy barriers. However, the resonance stability of the 2-butene 1,4-diradical makes its formation the more thermodynamically favorable pathway. It is worth noting that formation of the 2-butene 1,4-diradical is a bimolecular reaction, requiring 1 mol of ethylene for each mole of cyclobutane reacted; thus, it will exhibit greater pressure dependency than the unimolecular decomposition route that produces tetramethylene. Our proposed mechanism for the formation of cyclobutene also provides a source for the small concentrations of ethane consistently observed in our experimental results.

In Reactions 7 and 8, we have explored the free-radical addition of ethylene to both tetramethylene and to the 2-butene 1,4-diradical, giving hexamethylene and a 2-hexene 1,6-diradical, respectively. While we have only reported the first step of the chain-growth reactions involving tetramethylene and 2-butene 1,4-diradical, it is reasonable to assume that rapid growth of diradical chains will occur through free-radical polymerization and that this chain-growth will proceed with similar energetic requirements.

The instability of diradical intermediates is demonstrated clearly by the facile conversion of hexamethylene to 1-hexene. As seen in Figure S10, this conversion is highly exergonic and proceeds via a small free energy barrier. The 1-hexene produced from this reaction can participate analogously to the reaction pathway outlined in Reaction 12, producing a 2-hexene 1,6-diradical and ethane.

An alternative means of stabilizing the diradical intermediates is through hydrogen atom abstraction reactions between two diradical compounds. One example, Reaction 10, is the abstraction of a hydrogen atom from the second carbon of one hexamethylene to the end chain radical site of another hexamethylene, yielding an *n*-hexyl radical and a hex-5-enyl radical. The second example of a hydrogen atom abstraction reaction in this study is Reaction 11, occurring between the 2-hexene 1,6-diradical and 1-hexene. Abstraction from the allylic site of 1-hexene was chosen owing to the resonance stabilization of the neighboring double bond. Similarly, the nonallylic radical site of the 2-hexene 1,6-diradical was saturated with the abstracted hydrogen atom as the radical position at the other end of the chain is resonance stabilized.

Regardless of the formation pathway, the four monoradical species generated from the hydrogen atom abstraction reactions can participate in free radical polymerization reactions with ethylene, producing oligomeric polyethylene type species. The length of the growing carbon chains is dictated by an interplay of polymerization and cracking reactions. As seen by the changes in the MW distribution in Figure 1, this interplay of chain growth and cracking is sensitive to reaction temperature and pressure. Such reactions have been discussed at length elsewhere, and their roles in the thermal chemistry of polyolefins are well understood. Of particular interest to this work are β -scission reactions (see Figure 10), a midchain cleavage reaction that generates a smaller end-chain radical and a terminal alkene. In the case of a 2-hexyl radical, which can form via a 1,5-H shift from an n-



Figure 10. β-Scission reaction of a midchain radical (2-hexyl) to yield an end-chain radical (n-propyl) and a terminal alkene (propylene).

hexyl radical, the resulting β -scission products are an n-propyl radical and propylene. Likewise, a 1,4-H shift from an n-hexyl radical would yield a 3-hexyl radical, which could undergo β -scission to produce an ethyl radical and 1-butene.

The oligomerization of ethylene and subsequent generation of unsaturated products through cracking reactions represents the end of the initiation phase. Up to this point, all pathways are dependent on the bimolecular reactions of ethylene to form the diradical species. These reactions have very high activation free energies. Consequently, the concentration of all radical intermediates will start low, and the rate of oligomerization will be severely limited.

The terminal alkenes that are formed through β -scission reactions are able to participate in a lower energy radical-forming pathway akin to Reaction 12. The dehydrogenation of 1-butene by ethylene gives butadiene and ethane. This is followed by formation of the 2-butene 1,4-diradical generated in our earlier reactions. The free energy barrier for the first step is 54.6 kcal mol⁻¹, and for the second it is 53.0 kcal mol⁻¹. Both these values are significantly lower than any of the bimolecular ethylene reactions that were necessary for initial diradical formation. While not shown explicitly, we have observed that any unsaturated functionality within a chain is able to dehydrogenate another chain. We therefore posit that unsaturated chains of all observed lengths may be formed through these hydrogenation/dehydrogenation reactions.

Figure 11 provides a summary of the proposed oligomerization reaction pathways. The reactions that form part of the initiation pathways are shown with black arrows, while the secondary phase pathways are shown with green arrows. While not an exhaustive description of possible reactions, our computational study clearly supports a two-phase oligomerization of ethylene. High energy barrier bimolecular reactions of ethylene are required to generate the initial free radicals necessary for free radical oligomerization. Growing monoradical oligomer chains can then be subject to thermal cracking such as β -scission, yielding shorter-chain free radicals and unsaturated terminal alkenes among other species. The formation of these terminal alkenes allows for the generation of free radicals through lower energy pathways when compared against the bimolecular ethylene reactions. This more facile formation of free radicals will promote ethylene oligomerization at a much higher rate than during the initiation phase.

In contrast to ethylene, the thermal chemistry of propylene and 1-hexene reveal major differences. Propylene results in mostly the C₆ oligomer, which is the opposite of ethylene, shown to produce mostly propylene at the same conditions. Furthermore, propylene produces both branched and linear C₄, whereas ethylene makes linear C4. Propylene also gives rise to large amounts (>10 mol %) of methane at 500 °C (Figure S15), whereas ethylene does not. In contrast, a similarity of both ethylene and propylene reactions was the fact that 1hexene was a minor C₆ isomer. It comprised less than 10% of all C₆, which also contained some skeletal and/or cyclic isomers. For 1-hexene cracking, the C4 and C5 isomers resembled those of propylene much more closely than ethylene, with the presence of branched C₄ and C₅. Thus, in general, propylene and 1-hexene tend to produce more branched C₄, whereas ethylene favors linear C₄.

The reaction kinetics further highlight the dissimilarity between ethylene and propylene thermal reactions. Propylene was first-order with a lower activation energy of 29.9 kcal mol^{-1} from 410 to 500 °C. The lower overall activation energy

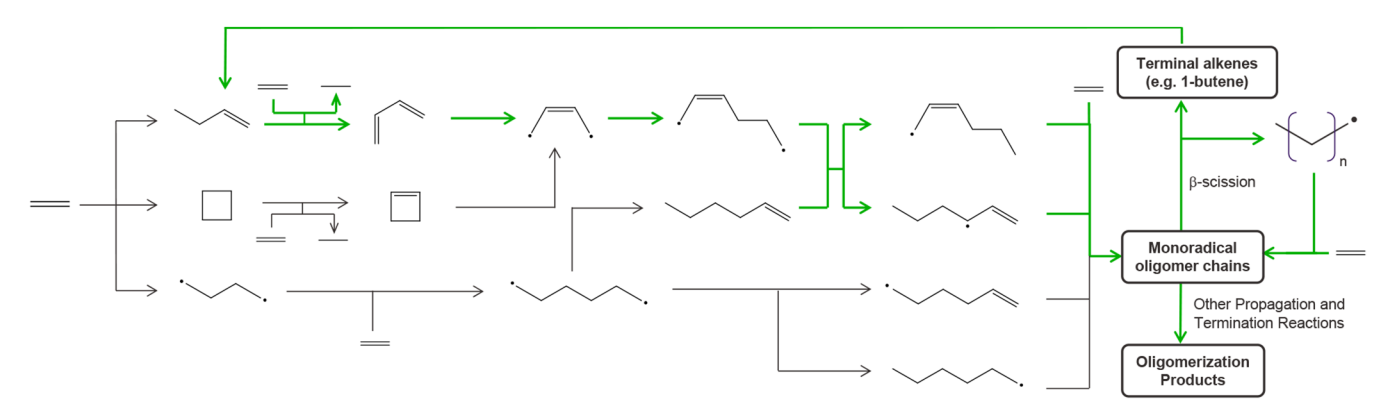


Figure 11. General scheme for the two-phase thermal oligomerization of ethylene.

is consistent with the observed higher rate of propylene conversion at 400 $^{\circ}$ C and 1.5 bar but higher rate of ethylene conversion at 500 $^{\circ}$ C and 1.5 bar. Additionally, the second-order pressure dependence results in high ethylene conversion rates at higher ethylene pressures as well as a more severe drop-off in rate as the pressure decreases below atmospheric. This observation is consistent with conclusions by previous workers that ethylene is the easiest olefin to polymerize thermally at high pressures. 21,33

The nature of the C–H bond strengths in ethylene and propylene are quite different. Ethylene contains four vinyl C–H bonds, which have a homolytic bond dissociation energy (BDE) of about 111 kcal mol⁻¹.⁸² Propylene, in contrast, possesses three allylic C–H bonds, which are much weaker (BDE = 89 kcal mol⁻¹) due to the resulting resonance stabilization that occurs for the allyl radical. Thus, the disparate chemical bond strengths of ethylene and propylene also suggest that their behavior in thermal reactions should be different, which is the case.

The extrapolated rates of 1-hexene cracking and isomerization at its experimentally observed concentration in the products, shown in Table S2, demonstrate strong evidence that 1-hexene cracking is not responsible for the observed nonoligomer products in either the reactions of ethylene or of propylene. This result indicates that the MW distributions are controlled by the propagation reactions of reactive free radical intermediates rather than degradation of stable C₆ products. The relative hexene isomerization rate, however, is at the same order of magnitude of the conversion rate of both ethylene and propylene to products and could be competitive with other routes leading to isomerization such as 1,4- and 1,5-hydrogen shifts.

5. CONCLUSIONS

Our in-depth study of the chemistry of ethylene thermal oligomerization to liquids has demonstrated several important characteristics. Below 500 °C and above atmospheric pressure, the reaction is second-order with a temperature-dependent overall activation energy, spanning 39.4 to 58.3 kcal mol $^{-1}$. Nonoligomer products are formed under all conditions, but these are not accompanied by formation of more than about 1 mol % each of methane and ethane. The $\rm C_4$ and $\rm C_5$ products are highly linear, with a strong preference for the terminal olefin. The free radical oligomerization appears to initiate by a two-phase process, with the likely formation of diradical intermediates. In the first phase, ethylene can react to form 1-butene or cyclobutane, in addition to tetramethylene. The

reaction to form vinyl and ethyl radicals proceeds with a considerably higher free energy barrier. Following several subsequent reaction steps such as cyclobutane cracking, ethylene addition, and hydrogen transfer, a second initiation phase can occur with more facile free radical generation due to the presence of unsaturated products which can hydrogenate ethylene and form conjugated diradicals.

The thermal reactions of propylene are very different than ethylene, displaying first-order kinetics with an activation energy of about 29.9 kcal mol⁻¹. The selectivity to nonoligomers is small compared to the dimer C₆ product, and many branched C4 and C5 products result in contrast to ethylene. The C₆ products for both ethylene and propylene reactions, however, are highly distributed among many isomers including some skeletal isomers and/or cyclic products. 1-Hexene is converted efficiently to other C₆ isomers in the almost complete absence of methane formation below 400 $^{\circ}$ C. Decomposition to C_2 – C_8 olefins occurs at a rate about 2–3 orders of magnitude slower than isomerization. The formation of C₃H₆ from C₂H₄, which occurs at very low conversion, does not occur by cracking of 1-hexene but instead as the result of a complex family of initiation and propagation steps of reactive radical polyethylene chains.

ASSOCIATED CONTENT

Supporting Information

The Supporting Information is available free of charge at https://pubs.acs.org/doi/10.1021/acs.iecr.2c02172.

Reactor temperature profiles, olefin conversion versus space velocity plots, sample GC chromatograms, images of transition states, DFT free energy profiles, propylene reaction product distributions, and 1-hexene product distributions (PDF)

AUTHOR INFORMATION

Corresponding Authors

Linda J. Broadbelt — Department of Chemical and Biological Engineering, Northwestern University, Evanston, Illinois 60208, United States; Orcid.org/0000-0003-4253-592X; Email: broadbelt@northwestern.edu

Jeffrey T. Miller — Davidson School of Chemical Engineering, Purdue University, West Lafayette, Indiana 47907, United States; orcid.org/0000-0002-6269-0620; Email: jeffreyt-miller@purdue.edu

Authors

- Matthew A. Conrad Davidson School of Chemical Engineering, Purdue University, West Lafayette, Indiana 47907, United States
- Alexander Shaw Department of Chemical and Biological Engineering, Northwestern University, Evanston, Illinois 60208, United States
- Grant Marsden Department of Chemical and Biological Engineering, Northwestern University, Evanston, Illinois 60208, United States

Complete contact information is available at: https://pubs.acs.org/10.1021/acs.iecr.2c02172

Notes

The authors declare no competing financial interest.

ACKNOWLEDGMENTS

This paper is based upon work supported primarily by the National Science Foundation (NSF) under GRFP grant number DGE-1842165 and Cooperative Agreement No. EEC-1647722. Any opinions, findings, and conclusions or recommendations expressed in this material are those of the author(s) and do not necessarily reflect the views of the National Science Foundation. This work used the Extreme Science and Engineering Discovery Environment (XSEDE), which is supported by National Science Foundation grant number ACI-1053575.

REFERENCES

- (1) Bell, A. T.; Alger, M. M.; Flytzani-Stephanopoulos, M.; Gunnoe, T. B.; Lercher, J. A.; Stevens, J.; Alper, J.; Tran, C. The Changing Landscape of Hydrocarbon Feedstocks for Chemical Production: Implications for Catalysis: Proceedings of a Workshop; The National Academies Press: Washington, DC, 2016.
- (2) Nalley, S.; LaRose, A. Annual Energy Outlook 2021; Press Release; U.S. Energy Information Administration: Washington, DC, 2021
- (3) Ridha, T.; Li, Y.; Gençer, E.; Siirola, J.; Miller, J.; Ribeiro, F.; Agrawal, R. Valorization of Shale Gas Condensate to Liquid Hydrocarbons through Catalytic Dehydrogenation and Oligomerization. *Processes* **2018**, *6* (9), 139.
- (4) Nicholas, C. P. Applications of Light Olefin Oligomerization to the Production of Fuels and Chemicals. *Appl. Catal., A* **2017**, 543, 82–97.
- (5) Ghashghaee, M. Heterogeneous Catalysts for Gas-Phase Conversion of Ethylene to Higher Olefins. *Rev. Chem. Eng.* **2018**, 34 (5), 595–655.
- (6) Sydora, O. L. Selective Ethylene Oligomerization. *Organometallics* **2019**, 38 (5), 997–1010.
- (7) Olivier-Bourbigou, H.; Breuil, P. A. R.; Magna, L.; Michel, T.; Espada Pastor, M. F.; Delcroix, D. Nickel Catalyzed Olefin Oligomerization and Dimerization. *Chem. Rev.* **2020**, *120* (15), 7919–7983.
- (8) Sanati, M.; Hörnell, C.; Järäs, S. G. The Oligomerization of Alkenes by Heterogeneous Catalysts. *Catalysis* **2007**, *14*, 236–288.
- (9) McGuinness, D. S. Olefin Oligomerization via Metallacycles: Dimerization, Trimerization, Tetramerization, and Beyond. *Chem. Rev.* **2011**, *111* (3), 2321–2341.
- (10) Al-Sherehy, F. A. IFP-SABIC Process for the Selective Ethylene Dimerization to Butene-1. *Stud. Surf. Sci. Catal.* **1996**, *100*, 515–523.
- (11) Speiser, F.; Braunstein, P.; Saussine, L. Catalytic Ethylene Dimerization and Oligomerization: Recent Developments with Nickel Complexes Containing P, N-Chelating Ligands. *Acc. Chem. Res.* **2005**, 38 (10), 784–793.
- (12) Lutz, E. F. Shell Higher Olefins Process. *J. Chem. Educ.* **1986**, 63 (3), 202.

- (13) Freitas, E. R.; Gum, C. R. Shell's Higher Olefins Process. *Chem. Eng. Prog.* **1979**, *75*, 73–76.
- (14) Finiels, A.; Fajula, F.; Hulea, V. Nickel-Based Solid Catalysts for Ethylene Oligomerization a Review. *Catal. Sci. Technol.* **2014**, *4* (8), 2412–2426.
- (15) Ipatieff, V. N.; Pines, H. Polymerization of Ethylene Under High Pressures in the Presence of Phosphoric Acid. *Ind. Eng. Chem.* 1935, 27 (11), 1364–1369.
- (16) Quann, R. J.; Green, L. A.; Tabak, S. A.; Krambeck, F. J. Chemistry of Olefin Oligomerization over ZSM-5 Catalyst. *Ind. Eng. Chem. Res.* **1988**, 27 (4), 565–570.
- (17) Chang, C. D. The New Zealand Gas-to-Gasoline Plant: An Engineering Tour de Force. *Catal. Today* **1992**, *13* (1), 103–111.
- (18) Garwood, W. E. Conversion of C₂-C₁₀ Olefins to Higher Olefins over Synthetic Zeolite ZSM-5. Symp. Adv. Zeolite Chem. 1982, 563–575.
- (19) Dunstan, A. E.; Hague, E. N.; Wheeler, R. V. Symposium on Hydrocarbon Decomposition Thermal Treatment of Gaseous Hydrocarbons I. Laboratory Scale Operation. *Ind. Eng. Chem.* **1934**, *26* (3), 307–314.
- (20) Frolich, P. K.; Wiezevich, P. J. Symposium on the Chemistry of Gaseous Hydrocarbons Cracking and Polymerization of Low Molecular Weight Hydrocarbons. *Ind. Eng. Chem.* **1935**, 27 (9), 1055–1062.
- (21) Sullivan, F. W.; Ruthruff, R. F.; Kuentzel, W. E. Pyrolysis and Polymerization of Gaseous Paraffins and Olefins. *Ind. Eng. Chem.* **1935**, *27* (9), 1072–1077.
- (22) Wagner, C. R. Production of Gasoline by Polymerization of Olefins. *Ind. Eng. Chem.* **1935**, 27 (8), 933–936.
- (23) Maschwitz, P. A.; Henderson, L. M. Polymerization of Hydrocarbon Gases to Motor Fuels. *Adv. Chem.* **1951**, *5*, 83–96.
- (24) Asinger, F. The Working Up of Lower, Normally Gaseous Paraffins and Mono-Olefins to Give Carburetor Fuels. In *Mono-Olefins*; Elsevier, 1968; pp 414–505.
- (25) Bondt, N.; Deiman, J. R.; van Troostwyk, P.; Lauwerenburg, A. On Three Different Species of Carbonaceous Hydrogen Gas, Removed from Ether and Alcohol by Different Processes. *Ann. Chim. Phys.* **1797**, *21*, 48–71.
- (26) Henry, W.; Dalton, J. XXVI. Experiments on Ammonia, and an Account of a New Method of Analyzing It, by Combustion with Oxygen and Other Gases; in a Letter to Humphry Davy, Esq. Sec. R. S. &c. from William Henry, M.D., F. R. S. V. P. of the Lit and Phil Society, and Physician to the Infirmary, at Manchester. *Philos. Trans. R. Soc.* **1809**, 99, 430–449.
- (27) Day, D. T. On the Changes Effected by Heat in the Constitution of Ethylene. Am. Chem. J. 1886, 8 (3), 153–167.
- (28) Norton, L. M.; Noyes, A. A. On the Action of Heat upon Ethylene. *Am. Chem. J.* **1886**, 8 (1), 362–364.
- (29) Bone, W. A.; Coward, H. F. CXVII.—The Thermal Decomposition of Hydrocarbons. Part I. [Methane, Ethane, Ethylene, and Acetylene.]. *J. Chem. Soc., Trans.* 1908, 93 (0), 1197–1225.
- (30) Ipatieff, V. N. Catalytic Reactions at High Pressures and Temperatures: Influence of Pressure on the Course of Catalysis. *Zh. Russ. Fiz. Khim.* **1906**, 63–75.
- (31) Ipatieff, V. N. Polymerization of Ethylene Hydrocarbons at High Temperatures and Pressures. *Ber. Dtsch. Chem. Ges.* **1911**, 44 (3), 2978–2987.
- (32) Egloff, G. Polymer Gasoline. Ind. Eng. Chem. 1936, 28 (12), 1461–1467.
- (33) Schmerling, L.; Ipatieff, V. N. The Mechanism of the Polymerization of Alkenes. *Adv. Catal.* **1950**, *2*, 21–80.
- (34) Fawcett, E. W.; Gibson, R. O.; Perrin, M. W. Polymerization of Olefins. US2,153,553, April 11, 1939.
- (35) Laird, R. K.; Morrell, A. G.; Seed, L. The Velocity of Ethylene Polymerization at High Pressures. *Discuss. Faraday Soc.* **1956**, 22, 126–137.
- (36) Woodbrey, J. C.; Ehrlich, P. The Free Radical, High Pressure Polymerization of Ethylene. II. The Evidence for Side Reactions from

- Polymer Structure and Number Average Molecular Weights. J. Am. Chem. Soc. 1963, 85 (11), 1580–1584.
- (37) Buback, M. The High Pressure Polymerization of Pure Ethylene. *Makromol. Chem.* **1980**, *181* (2), 373–382.
- (38) Buback, M. Spectroscopic Investigation of the High Pressure Ethylene Polymerization. Z. Naturforsch., A 1984, 39 (4), 399–411.
- (39) Scelta, D.; Ceppatelli, M.; Bini, R. Pressure Induced Polymerization of Fluid Ethylene. *J. Chem. Phys.* **2016**, *145* (16), 164504
- (40) Citroni, M.; Ceppatelli, M.; Bini, R.; Schettino, V. High-Pressure Reactivity of Propene. J. Chem. Phys. 2005, 123 (19), 194510.
- (41) Szwarc, M. The Kinetics of the Thermal Decomposition of Propylene. J. Chem. Phys. 1949, 17 (3), 284–291.
- (42) Ingold, K. U.; Stubbs, F. J. 382. The Kinetics of the Thermal Decomposition of Olefins. Part I. Propylene. *J. Chem. Soc.* 1951, 1749–1755.
- (43) Molera, M. J.; Stubbs, F. J. 75. The Kinetics of the Thermal Decomposition of Olefins. Part II. *J. Chem. Soc.* **1952**, 381–391.
- (44) Silcocks, C. G. The Kinetics of the Thermal Decomposition and Polymerization of Ethane and Ethylene. *Proc. R. Soc. London A* **1956**, 233 (1195), 465–479.
- (45) Dahlgren, G.; Douglas, J. E. Kinetics of the Thermal Reactions of Ethylene. J. Am. Chem. Soc. 1958, 80 (19), 5108-5110.
- (46) Laidler, K. J.; Wojciechowski, B. W. Kinetics of the Thermal Decomposition of Propylene, and of Propylene-Inhibited Hydrocarbon Decompositions. *Proc. R. Soc. London A* **1960**, 259 (1297), 257–266.
- (47) Skinner, G. B.; Sokoloski, E. M. Shock Tube Experiments on the Pyrolysis of Ethylene. *J. Phys. Chem.* **1960**, *64* (8), 1028–1031.
- (48) Taniewski, M. Investigations on the Thermal Decomposition of Olefins. *Proc. R. Soc. London A* **1962**, 265 (1323), 519–537.
- (49) Amano, A.; Uchiyama, M. Mechanism of the Pyrolysis of Propylene: The Formation of Allene. *J. Phys. Chem.* **1964**, *68* (5), 1133–1137.
- (50) Benson, S. W.; Haugen, G. R. Mechanisms for Some High-Temperature Gas-Phase Reactions of Ethylene, Acetylene, and Butadiene. *J. Phys. Chem.* **1967**, *71* (6), 1735–1746.
- (51) Kallend, A. S.; Purnell, J. H.; Shurlock, B. C. The Pyrolysis of Propylene. *Proc. R. Soc. London A* **1967**, 300 (1460), 120–139.
- (52) Boyd, M. L.; Wu, T.-M.; Back, M. H. Kinetics of the Thermal Reactions of Ethylene. Part I. Can. J. Chem. 1968, 46 (14), 2415–2426.
- (53) Boyd, M. L.; Back, M. H. Kinetics of the Thermal Reactions of Ethylene. Part II. Ethylene–Ethane Mixtures. *Can. J. Chem.* **1968**, *46* (14), 2427–2433.
- (54) Halstead, M. P.; Quinn, C. P. Pyrolysis of Ethylene. *Trans. Faraday Soc.* **1968**, *64*, 103–118.
- (55) Kunugi, T.; Sakai, T.; Soma, K.; Sasaki, Y. Kinetics and Mechanism of Thermal Reaction of Ethylene. *Ind. Eng. Chem. Fundam.* **1969**, 8 (3), 374–383.
- (56) Kunugi, T.; Sakai, T.; Soma, K.; Sasaki, Y. Thermal Reaction of Propylene. Kinetics. *Ind. Eng. Chem. Fundam.* **1970**, 9 (3), 314–318.
- (57) Simon, M.; Back, M. H. Kinetics of the Thermal Reactions of Ethylene. *Can. J. Chem.* **1969**, 47 (2), 251–255.
- (58) Back, M. H. Mechanism of the Bimolecular Reactions of Ethylene and Propylene. *Int. J. Chem. Kinet.* **1970**, 2 (5), 409–418.
- (59) Simon, M.; Back, M. H. Kinetics of the Pyrolysis of Propylene. Part I. Can. J. Chem. 1970, 48 (2), 317–325.
- (60) Simon, M.; Back, M. H. Kinetics of the Pyrolysis of Propylene. Part II. Can. J. Chem. 1970, 48 (21), 3313–3319.
- (61) Back, M. H.; Martin, R. The Thermal Reactions of Ethylene at 500°C in the Presence and Absence of Small Quantities of Oxygen. *Int. J. Chem. Kinet.* **1979**, *11* (7), 757–774.
- (62) Ayranci, G.; Back, M. H. Kinetics of the Bimolecular Initiation Process in the Thermal Reactions of Ethylene. *Int. J. Chem. Kinet.* **1981**, *13* (9), 897–911.

- (63) Ayranci, G. Kinetics of the Bimolecular Initiation Process in the Thermal Reactions of Ethylene. Doctoral Thesis, University of Ottawa. 1982.
- (64) Quick, L. M.; Knecht, D. A.; Back, M. H. Kinetics of the Formation of Cyclobutane from Ethylene. *Int. J. Chem. Kinet.* **1972**, 4 (1), 61–68.
- (65) Pease, R. N. Kinetics of the Polymerization of Ethylene at Pressures above One Atmosphere. *J. Am. Chem. Soc.* **1931**, *53* (2), 613–619.
- (66) Storch, H. H. Kinetics of Ethylene Polymerization. *J. Am. Chem. Soc.* **1934**, *56* (2), 374–378.
- (67) Storch, H. H. Kinetics of Ethylene Polymerization. II. *J. Am. Chem. Soc.* **1935**, *57* (12), 2598–2601.
- (68) Pease, R. N. The Non-Catalytic Polymerization and Hydrogenation of Ethylene. J. Am. Chem. Soc. 1930, 52 (3), 1158–1164.
- (69) Douglas, J. E.; Rabinovitch, B. S.; Looney, F. S. Kinetics of the Thermal *Cis-Trans* Isomerization of Dideuteroethylene. *J. Chem. Phys.* **1955**, 23 (2), 315–323.
- (70) Hurd, C. D. Pyrolysis of Unsaturated Hydrocarbons. *Ind. Eng. Chem.* **1934**, 26 (1), 50–55.
- (71) Yaws, C. L. Thermophysical Properties of Superheated, Saturated, and Subcooled Fluids. In Yaws' Critical Property Data for Chemical Engineers and Chemists; Knovel, 2012.
- (72) Frisch, M. J.; Trucks, G. W.; Schlegel, H. B.; Scuseria, G. E.; Robb, M. A.; Cheeseman, J. R.; Scalmani, G.; Barone, V.; Petersson, G. A.; Nakatsuji, H.; Li, X.; Caricato, M.; Marenich, A. V.; Bloino, J.; Janesko, B. G.; Gomperts, R.; Mennucci, B.; Hratchian, H. P.; Ortiz, J. V.; Izmaylov, A. F.; Sonnenberg, J. L.; Williams-Young, D.; Ding, F.; Lipparini, F.; Egidi, F.; Goings, J.; Peng, B.; Petrone, A.; Henderson, T.; Ranasinghe, D.; Zakrzewski, V. G.; Gao, J.; Rega, N.; Zheng, G.; Liang, W.; Hada, M.; Ehara, M.; Toyota, K.; Fukuda, R.; Hasegawa, J.; Ishida, M.; Nakajima, T.; Honda, Y.; Kitao, O.; Nakai, H.; Vreven, T.; Throssell, K.; Montgomery, J. A., Jr.; Peralta, J. E.; Ogliaro, F.; Bearpark, M.; Heyd, J. J.; Brothers, E. N.; Kudin, K. N.; Staroverov, V. N.; Kobayashi, R.; Normand, J.; Raghavachari, K.; Rendell, A.; Burant, J. C.; Iyengar, S. S.; Tomasi, J.; Cossi, M.; Millam, J. M.; Klene, M.; Adamo, C.; Cammi, R.; Ochterski, J. W.; Martin, R. L.; Morokuma, K.; Farkas, O.; Foresman, J. B.; Fox, D. J. Gaussian 16, revision C.01; Gaussian, Inc.: Wallingford, CT, 2016.
- (73) Zhao, Y.; Truhlar, D. G. Density Functional for Spectroscopy: No Long-Range Self-Interaction Error, Good Performance for Rydberg and Charge-Transfer States, and Better Performance on Average than B3LYP for Ground States. *J. Phys. Chem. A* **2006**, *110* (49), 13126–13130.
- (74) Zhao, Y.; Truhlar, D. G. The M06 Suite of Density Functionals for Main Group Thermochemistry, Thermochemical Kinetics, Noncovalent Interactions, Excited States, and Transition Elements: Two New Functionals and Systematic Testing of Four M06-Class Functionals and 12 Other Functionals. *Theor. Chem. Acc.* **2008**, *120* (1–3), 215–241.
- (75) Weigend, F.; Ahlrichs, R. Balanced Basis Sets of Split Valence, Triple Zeta Valence and Quadruple Zeta Valence Quality for H to Rn: Design and Assessment of Accuracy. *Phys. Chem. Chem. Phys.* **2005**, 7 (18), 3297–3305.
- (76) Grimme, S.; Antony, J.; Ehrlich, S.; Krieg, H. A Consistent and Accurate *Ab Initio* Parametrization of Density Functional Dispersion Correction (DFT-D) for the 94 Elements H-Pu. *J. Chem. Phys.* **2010**, 132 (15), 154104.
- (77) Li, Y.-P.; Gomes, J.; Mallikarjun Sharada, S.; Bell, A. T.; Head-Gordon, M. Improved Force-Field Parameters for QM/MM Simulations of the Energies of Adsorption for Molecules in Zeolites and a Free Rotor Correction to the Rigid Rotor Harmonic Oscillator Model for Adsorption Enthalpies. *J. Phys. Chem. C* **2015**, *119* (4), 1840–1850.
- (78) Grimme, S. Supramolecular Binding Thermodynamics by Dispersion-Corrected Density Functional Theory. *Chem. Eur. J.* **2012**, *18* (32), 9955–9964.
- (79) Luchini, G.; Alegre-Requena, J.; IFunes; Rodríguez-Guerra, J.; Chen, J.; Paton, R. *Bobbypaton/GoodVibes: GoodVibes* v3.0.0, 2019.

- (80) Yu, H.; Zheng, J.; Truhlar, D. G. Unpublished data, 2015.
- (81) Rofer-DePoorter, C. K. A Comprehensive Mechanism for the Fischer-Tropsch Synthesis. *Chem. Rev.* **1981**, *81* (5), 447–474.
- (82) Loudon, G. M. Organic Chemistry, 5th ed.; Roberts and Co.: Greenwood Village, CO, 2009.
- (83) Quinn, C. P. Isomerization of Primary N-Alkyl Radicals in the Pyrolysis of Ethane. *Trans. Faraday Soc.* **1963**, *59*, 2543–2547.
- (84) Viskolcz, B.; Lendvay, G.; Körtvélyesi, T.; Seres, L. Intramolecular H Atom Transfer Reactions in Alkyl Radicals and the Ring Strain Energy in the Transition Structure. *J. Am. Chem. Soc.* **1996**, *118* (12), 3006–3009.
- (85) Viskolcz, B.; Lendvay, G.; Seres, L. Ab Initio Barrier Heights and Branching Ratios of Isomerization Reactions of a Branched Alkyl Radical. *J. Phys. Chem. A* **1997**, *101* (38), 7119–7127.
- (86) Tsang, W.; Walker, J. A.; Manion, J. A. The Decomposition of Normal Hexyl Radicals. *Proc. Combust. Inst.* **2007**, 31 (1), 141–148.
- (87) Cheng, J.; Gao, Y.; Li, X.; You, X.; Zou, C. Reaction Kinetics of Hydrogen Shift Isomerization of 1-Hexyl Radicals. *Fuel* **2020**, *278*, 118221.
- (88) Roedel, M. J. The Molecular Structure of Polyethylene. I. Chain Branching in Polyethylene during Polymerization. *J. Am. Chem. Soc.* **1953**, 75 (24), 6110–6112.
- (89) Bryant, W. M. D.; Voter, R. C. The Molecular Structure of Polyethylene. II. Determination of Short Chain Branching. *J. Am. Chem. Soc.* **1953**, 75 (24), 6113–6118.
- (90) Elias, H.-G. Free-Radical Polymerization. In *Macromolecules*; Wiley-VCH Verlag GmbH: Weinheim, Germany, 2014; pp 309–367.
- (91) Yamada, B.; Zetterlund, P. B. General Chemistry of Radical Polymerization. In *Handbook of Radical Polymerization*; Matyjaszewski, K., Davis, T. P., Eds.; John Wiley & Sons, Inc.: Hoboken, NJ, U, 2002; pp 117–186.

☐ Recommended by ACS

Heterocene Catalysts and Reaction Temperature Gradient in Dec-1-ene Oligomerization for the Production of Low Viscosity PAO Base Stocks

Ilya E. Nifant'ev, Pavel V. Ivchenko, *et al.*MARCH 29, 2023
INDUSTRIAL & ENGINEERING CHEMISTRY RESFARCH

READ 🗹

Thermodynamic and Mechanistic Analyses of Direct CO₂ Methylation with Toluene to *para*-Xylene

Yong Yang, Dongqiang Zhang, et al.

JUNE 21, 2023 ACS OMEGA

READ 🗹

First-Principles Analysis of Ethylene Oligomerization on Single-Site Ga³⁺ Catalysts Supported on Amorphous Silica

Yinan Xu, Jeffrey Greeley, et al.

APRIL 21, 2022 ACS CATALYSIS

READ [7

Role of Bifunctional Ru/Acid Catalysts in the Selective Hydrocracking of Polyethylene and Polypropylene Waste to Liquid Hydrocarbons

Julie E. Rorrer, Yuriy Román-Leshkov, et al.

OCTOBER 31, 2022

ACS CATALYSIS

READ 🗹

Get More Suggestions >